

Topological quantum phase transition in an $S=2$ spin chain

Jiadong Zang,¹ Hong-Chen Jiang,^{2,3} Zheng-Yu Weng,³ and Shou-Cheng Zhang⁴

¹Department of Physics, Fudan University, Shanghai 200433, China

²Microsoft Research, Station Q, University of California, Santa Barbara, California 93106, USA

³Center for Advanced Study, Tsinghua University, Beijing 10084, China

⁴Department of Physics, Stanford University, Stanford, California 94305, USA

(Received 4 February 2010; revised manuscript received 4 June 2010; published 24 June 2010)

We construct a model Hamiltonian for $S=2$ spin chain, where a variable parameter α is introduced. The edge spin is $S=1$ for $\alpha=0$ and $S=3/2$ for $\alpha=1$. Due to the topological distinction of the edge states, these two phases must be separated by one or several topological quantum phase transitions. We have studied the quantum phase transition by density matrix renormalization group calculation and proposed a phase diagram for this model.

DOI: [10.1103/PhysRevB.81.224430](https://doi.org/10.1103/PhysRevB.81.224430)

PACS number(s): 05.30.Rt, 75.10.Jm, 75.10.Pq

I. INTRODUCTION

Recently, investigations of topological phases and phase transitions has attracted great attention in condensed-matter physics.¹ The quantum-Hall state² is the first example of a topological state of quantum matter, with a fully gap ground state in the bulk, and gapless excitations at the edge. The chiral edge state is a holographic mirror of bulk topology.³ In the recently discovered time-reversal invariant topological insulators,^{4,5} helical edge states are confined at the edge by the bulk energy gap, and states with opposite spins counter-propagate. In the case of the quantum spin-Hall state realized in HgTe quantum wells, the topologically trivial and non-trivial states are separated by a topological quantum phase transition, tunable by the thickness of the quantum well.

Quantum spin chain is another example where topological quantum phase transition is found. The low-energy dynamics of one-dimensional large-spin Heisenberg antiferromagnet can be described as $O(3)$ nonlinear sigma model.⁶ Half-integer-spin chains are generally gapless while integer spin chains are gapped; they are described by the $O(3)$ nonlinear sigma model with and without the topological term. This distinction bears strong similarity to the topological insulators, which is distinct from the conventional insulators by the presence of a topological term.⁷

In this paper, we investigate a spin-2 chain model with two topologically distinct, transactionally invariant ground states. One model has edge state $S=1$ while the other model has edge spin $S=3/2$. The Berry's phase associated with the edge spins differ by π . The square of the time reversal operator T gives $T^2=1$ for the first case whereas it gives $T^2=-1$ in the second case. Due to this topological difference, the two ground states must be separated by one or several topological quantum phase transitions where the spin gap closes.

This paper is constructed as follows. In the next section, we will review two exact solvable quantum spin model in one dimension. Some materials can be systematically found in a brilliant work by Tu *et al.*⁸ Afterward, our new model Hamiltonian is presented according to the topological argument. Corresponding numerical results are shown in the third section, where phase diagram is discussed as well. Conclusions are drawn in the end.

II. MODEL HAMILTONIAN

Our starting point is an integer spin model introduced by Affleck, Kennedy, Lieb, and Tasaki, namely, the AKLT model.^{9,10} It is proved that the AKLT model has a unique infinite volume ground state with an exponential decay spin-spin correlation.¹⁰ In agreement with the Haldane conjecture,¹¹ the excitation gap of AKLT model is nonzero. The ground state of AKLT model can be written down exactly in terms of Schwinger bosons

$$|\Psi^{\text{AKLT}}\rangle = \prod_{\langle ij \rangle} (a_i^\dagger b_j^\dagger - b_i^\dagger a_j^\dagger)^S |0\rangle, \quad (1)$$

where S stands for site spin, and a_i^\dagger, b_i^\dagger are creation operators of Schwinger bosons at the i th site. This ground state can be rephrased in a pictorial form. The spin-2 AKLT ground state can be schematically shown in Fig. 1, where the circles stand for sites on the chain. Each spin-2 can be decomposed into totally symmetric combinations of four spin-1/2 states and each state is represented by a solid dot in the figure. Two pairs of neighboring dots form singlet states, shown in solid bonds. These bonds are usually called *valence bonds*, and in this sense, AKLT ground state is usually referred as *valence bond state*. It is proved rigorously that this ground state is unique under this periodic boundary condition. Due to the symmetric intrasite coupling and antisymmetric intersite coupling, the parent Hamiltonian of this ground state is given by

$$H^{\text{AKLT}} = \sum_{\langle ij \rangle} K_3 P_3(\mathbf{S}_i, \mathbf{S}_j) + K_4 P_4(\mathbf{S}_i, \mathbf{S}_j), \quad K_3, K_4 > 0, \quad (2)$$

where P_3 and P_4 are the projection operators onto the spin-3 and spin-4 subspaces, respectively. The positive coefficients



FIG. 1. (Color online) The sketch of spin-2 AKLT wave function. The circles represent sites and each spin-2 is decomposed into four spin-1/2 solid dots. Red lines connecting the dots stand for singlet states.

ensure the state in Eq. (1) to be the corresponding ground state.

In 1998, Scalapino, Zhang, and Hanke (SZH) introduced a SO(5) symmetric spin model¹² with an exact valence-bond ground state. The original motivation for the model is to illustrate the SO(5) theory of high T_c superconductivity, which unifies the antiferromagnetic and the d -wave superconducting phases.^{13,14} However, it was soon found later that the SO(5) symmetry can also be interpreted as an enhanced spin rotational symmetry.¹⁵ The SZH model contains five quantum states at each site, forming the vector representation of the SO(5) group. However, these five states can also be interpreted as the quantum states of the spin $S=2$ of the SO(3) spin chain. SZH presented an exact ground-state wave function expressed as a matrix product state of the Dirac Γ matrices and showed that the edge states of the SZH model are fourfold degenerate at each edge. Interpreted as an $S=2$ chain language, the edge spin contains $S=3/2$ spin quantum numbers. Following this work, more valence-bond states with higher symmetry groups have been constructed.^{8,16-19}

The basic idea of the SZH model is the following. The tensor product of two SO(5) spinor can be decomposed into SO(5) singlet, antisymmetric tensor, and symmetric traceless tensor, namely,

$$5 \times 5 = 1 + 10 + 14. \quad (3)$$

In analogy with the spin-1 AKLT model, the largest subspace is projected out, leading to the desired SZH model

$$H = J \sum_{\langle xy \rangle} P_{14}(xy), \quad J > 0. \quad (4)$$

Due to the Clifford algebra of the five Γ matrices: $\Gamma^a \Gamma^b = 2\delta^{ab} + 2i\Gamma^{ab}$, no symmetric traceless components are involved in the product of two Γ matrices. As a consequence

$$|\Psi^{\text{SZH}}\rangle = \sum_{m_1, \dots, m_N} \text{Tr}(\Gamma^{m_1} \Gamma^{m_2} \dots \Gamma^{m_N}) |m_1 m_2 \dots m_N\rangle \quad (5)$$

is the ground state of the above SZH model, where m is a vector label of the SO(5) group, which can also be interpreted as the $m_i = -2, -1, 0, 1, 2$ quantum numbers of $S=2$ spin chain.

Due to the relationships between the SO(5) and the SO(3) groups, there exists a natural deformation of the SZH model to an SU(2) spin-2 SZH model. The required map from SO(5) group onto SU(2) group with spin-2 is given by

$$10[\text{SO}(5)] = 3[\text{SO}(3)] \oplus 7[\text{SO}(3)], \quad (6)$$

$$14[\text{SO}(5)] = 5[\text{SO}(3)] \oplus 9[\text{SO}(3)]. \quad (7)$$

And therefore the SZH Hamiltonian deforms to

$$H^{\text{SZH}} = \sum_{\langle ij \rangle} J_2 P_2(\mathbf{S}_i, \mathbf{S}_j) + J_4 P_4(\mathbf{S}_i, \mathbf{S}_j), \quad J_2, J_4 > 0. \quad (8)$$

The ground state is unchanged up to an SO(5) rotation.

To see if the SZH state is gapped or not, we can evaluate the ground-state spin-correlation function. The correlation of matrix product state can be easily derived by the transfer matrix technique, given by

$$\langle S_1^\mu S_r^\mu \rangle = (\text{Tr } G^L)^{-1} \text{Tr}[Z(S^\mu) G^{r-2} Z(S^\mu) G^{L-r}], \quad (9)$$

where $\mu = x, y, z$.⁸ Define $g = \sum_m \Gamma^m |m\rangle$, then $G = g^\dagger \otimes g = \sum_m \Gamma^m \otimes \Gamma^m$, and $Z(S^\mu) = g^\dagger \otimes S^\mu g$. As it's an isotropic magnet, the correlation functions are the same in any directions. After some detail calculation, we derive $\langle S_1^x S_r^x \rangle = \langle S_1^y S_r^y \rangle = \langle S_1^z S_r^z \rangle = -20 \times 5^{-r}$ for integer $r > 1$. Therefore, the correlation length ξ of the SZH model equals to $1/\ln 5$. This finite correlation length indicates that the low-lying excitation in the SZH model is gapped, consistent with the Haldane conjecture.

It is interesting to note that the correlation function of the SZH model is negative definite with a correlation length $\xi = 1/\ln 5 \sim 0.61$. Consequently, the lattice constant is almost twice of the correlation length and the spins at neighboring sites correlate extremely weakly. On the other hand, according to Arovas *et al.*'s work,²⁰ the correlation length for spin-2 AKLT is $1/\ln 2$ which is roughly the lattice constant. Therefore, although AKLT model is also a strongly disordered antiferromagnet, the neighboring spins are closely correlated, leading to the conventional staggering correlation function, say, $S_1 S_r \propto (-1)^r 2^{-r}$.

Now we have two sets of models of one-dimensional spin-2 chain with exactly known Hamiltonians and ground-state wave functions. The differences between the AKLT and SZH model are not only the analytic forms as they appear but also the topological distinctions. The same as topological insulator, the bulk topology is relevant to the edge state of an open chain. For the spin-2 AKLT model, two solid dots at each edge remain free. Symmetrical combination of these two spin-1/2 dots results an edge spin with $S=1$. This boson-like edge state is consistent with large- N theory of SU(N) quantum antiferromagnets.²¹ However, the SZH model serves a complement of the large- N analysis. For an open chain, the SZH ground state is given by

$$|\Psi; i, j\rangle = \sum_{m_1, \dots, m_N} (\Gamma^{m_1} \Gamma^{m_2} \dots \Gamma^{m_N})_{ij} |m_1 m_2 \dots m_N\rangle. \quad (10)$$

It explicitly shows that at each edge, there are four degrees of freedom since the matrix product state is four dimensional. Therefore, the edge state of SZH model is spin-3/2, i.e., fermionlike. That is completely different from the AKLT model. As the edge state is protected by topology, and is robust under perturbation, the AKLT and SZH models belong to different topological classes. It can be easily understood from the Berry phase's language. Berry phase Φ_{BP} is the additional phase when the spin winds around, which relates to the expectation value of T^2 by $\exp(-i\Phi_{BP}) = \langle T^2 \rangle$, where T is the time reversal operator. It is well known that $T^2 = -1$ for half-integer spins such as $S=3/2$ while $T^2=1$ for integer spins such as $S=1$. As a consequence, the Berry phases of the two models under investigation differ by an angle of π . It is this difference that makes topological distinction of AKLT and SZH models. From another points of view, the edge spin determines the ground-state degeneracy²² and naturally serves as a topology index in analogy to fractional quantum Hall effect. These two models thus have different topology index due to different edge spins.

Given the topological distinction of the two ground states, we construct a model Hamiltonian interpolating between the AKLT and SZH models

$$H(\alpha) = (1 - \alpha)H^{\text{AKLT}} + \alpha H^{\text{SZH}}. \quad (11)$$

Without loss of generality, we set $J_2=K_3=1$ and $J_4=K_4=\beta$ in the following. As the edge state is robust unless the gap closes, there must exist one or several topological quantum phase transitions (TQPT) where the gap closes and reopens in the evolution of α from 0 to 1. This TQPT can be addressed by studying the behavior of energy spectrum and correlation function at each α .

III. NUMERICAL RESULTS

The *density matrix renormalization group* (DMRG) method is employed²³ in our study. For this purpose, it is helpful to rewrite the projection operators explicitly in terms of spin operators. Applying the identity

$$\mathbf{S}_i \cdot \mathbf{S}_j = \sum_{J=0}^{2S} \left[\frac{1}{2} J(J+1) - S(S+1) \right] P_J(ij) \quad (12)$$

one can easily get

$$P_2(ij) = \frac{1}{126} [-120(\mathbf{S}_i \cdot \mathbf{S}_j) - 14(\mathbf{S}_i \cdot \mathbf{S}_j)^2 + 7(\mathbf{S}_i \cdot \mathbf{S}_j)^3 + (\mathbf{S}_i \cdot \mathbf{S}_j)^4], \quad (13)$$

$$P_3(ij) = \frac{1}{360} [162(\mathbf{S}_i \cdot \mathbf{S}_j) - 7(\mathbf{S}_i \cdot \mathbf{S}_j)^2 - 10(\mathbf{S}_i \cdot \mathbf{S}_j)^3 - (\mathbf{S}_i \cdot \mathbf{S}_j)^4] + 1, \quad (14)$$

$$P_4(ij) = \frac{1}{2520} [90(\mathbf{S}_i \cdot \mathbf{S}_j) + 63(\mathbf{S}_i \cdot \mathbf{S}_j)^2 + 14(\mathbf{S}_i \cdot \mathbf{S}_j)^3 + (\mathbf{S}_i \cdot \mathbf{S}_j)^4]. \quad (15)$$

For present study, we keep $m=600-1000$ states in the DMRG block with more than 16 sweeps to get a converged result, and the truncation error is less than 10^{-7} in near the critical point, and much less than 10^{-10} away from the critical point. We make use of the open boundary condition (OBC) and the total number of sites is $N=600$. To check the finite-size effect of the system, we have studied the ground-state energy per site E_0/N and the absolute value of the corresponding second derivative $|d^2E/d\alpha^2|$ with respect to α , with system size $N=10-1000$ and $\beta=1$, as shown in Fig. 2. Such the ground-state energy E_0/N starts to converge and the sharp peak of $|d^2E_0/d\alpha^2|$ appears at $N \geq 60$. Besides the ground-state energy, we have also calculated the correlation functions and find that the finite-size effect can be neglected at $N \geq 600$. Therefore, in the following calculation, $N=600$ is adopted, for which the finite-size effect can be completely neglected.

Consistent with the discussion above, the existence of TQPT is clearly supported by the numerical calculation, as shown in Fig. 2. The second derivative of the ground energy

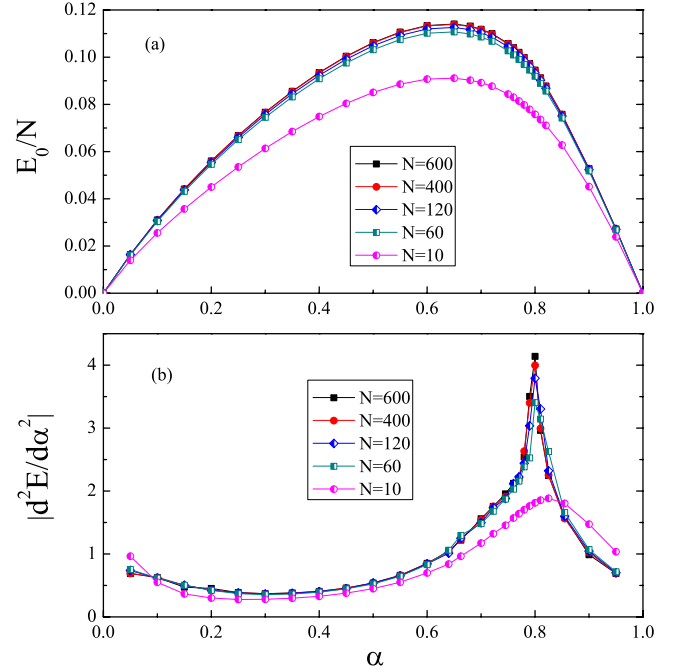


FIG. 2. (Color online) (a) Ground-state energy per site E_0/N and (b) the absolute value of its corresponding second derivative $|d^2E/d\alpha^2|$, as a function of α , got by DMRG with 600 states and $\beta=1.0$ at different system sizes.

has a sharp peak around $\alpha_c \approx 0.80$, which indicates the second order quantum phase transition addressed above. This is further confirmed by the real-space spin-spin correlation function, as shown in Fig. 3. At $\alpha=0$ and 1, the correlation function is exactly the same with the analytical result. When $\alpha < 0.80$, the correlation behaves similarly with the AKLT model, showing an oscillating behavior with respect the lattice separation. However, when $\alpha > 0.80$, the correlation behaves similarly with the SZH model, showing an negative-definite behavior. At the critical point, the correlation function undergoes a qualitative change from AKLT to SZH.

To get the ground-state phase diagram, we also calculate the peak position α_c of $|d^2E/d\alpha^2|$ as a function of β , as shown in Fig. 5. Above the red line, the system is topologically connected to SZH model and therefore belongs to the same topological class as SZH phase. One feature of this phase is translational symmetric and has spin-3/2 excitations on the edge. Similarly, the regions where α is small belong to the same topological class as AKLT phase. Translational symmetry is also respected but with spin-1 excitations on the edge.

However, one thing we should keep in mind that even the model Hamiltonian is translational invariant, spontaneous symmetry breaking is also possible. One well known example is the bilinear-biquadratic model for spin-1 chain whose Hamiltonian is also written in terms of local projections and translational invariant. However, the emergence of the dimerized phase is addressed in previous works.²⁴⁻²⁶ In order to quantitatively describe this issue, the following dimer order parameter:

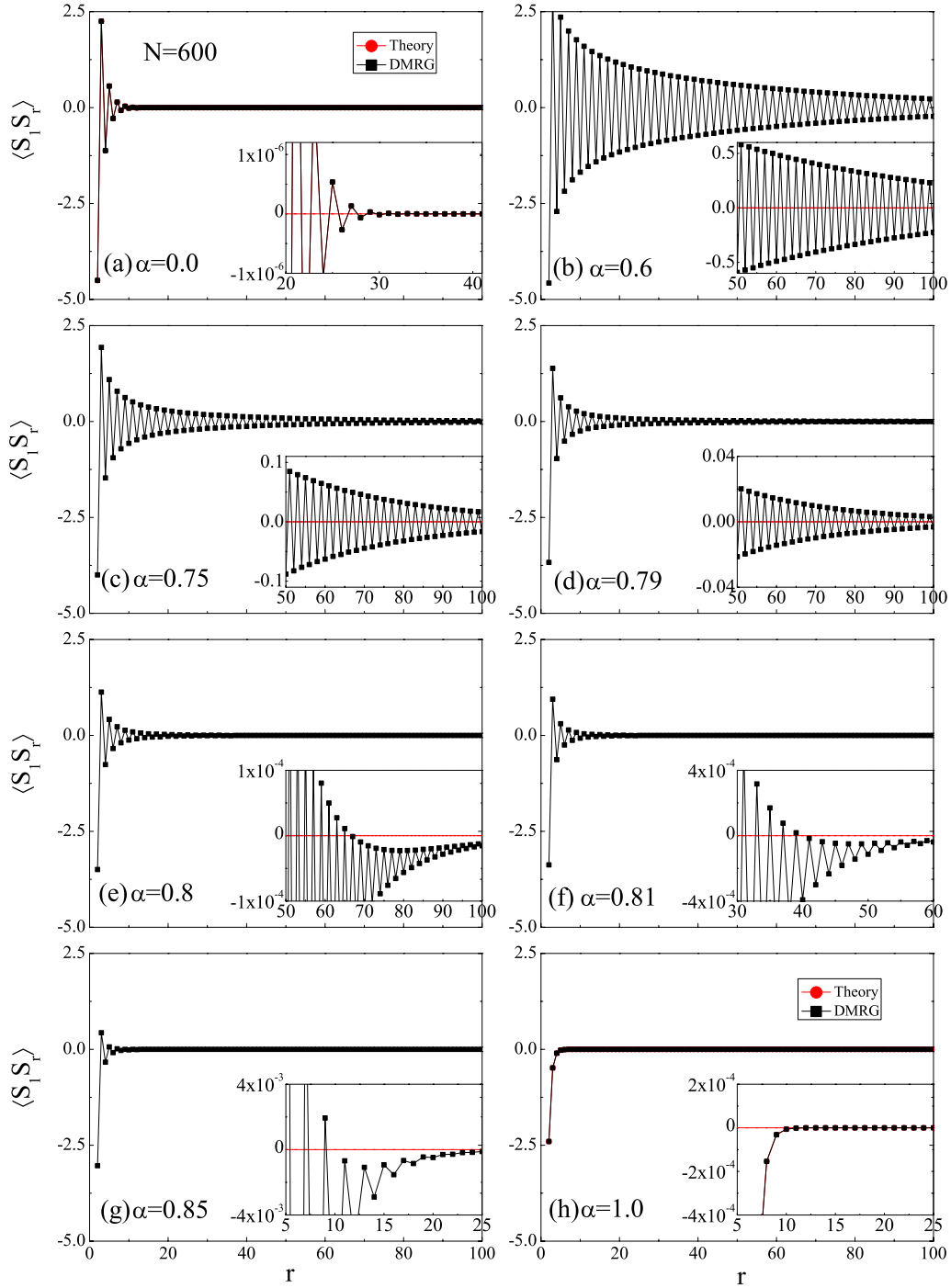


FIG. 3. (Color online) The real-space spin-spin correlation functions $\langle S_1 \cdot S_r \rangle$ at different α , obtained by the DMRG with $N=600$ and $\beta=1.0$.

$$D_\alpha = |\langle S_i S_{i+1} \rangle - \langle S_{i+1} S_{i+2} \rangle| \quad (16)$$

as a function of α is introduced, where i labels the center site in the spin chain so that one can minimize the possible finite-size effect induced by open boundary condition. In the calculation, the total site number N is set to be an even number to avoid potential ambiguity in the definition, in which case i is simply $N/2$. The indications of dimerization are plotted in Fig. 4. It is shown explicitly that dimerization appears with

proper choices of parameters α and β . One can rule out possible finite-size effect as the dimer order parameter does not scale with the system size N , shown in Fig. 4(a). When β decreases, the maximum amplitude of dimer order parameter decreases as well, and the dimerization expands less and less regions of α monotonously. At the critical point $\beta=0.27$, dimer order parameter vanishes for any α , and the corresponding dimerization phase shrinks as well. The system undergoes a quantum phase transition without spontaneous breaking of translational symmetry. During this phase transi-

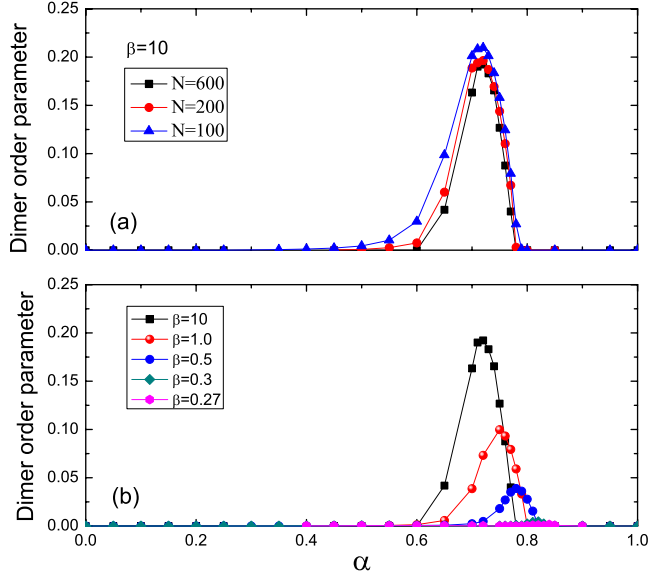


FIG. 4. (Color online) Dimer order parameters of the model Hamiltonian with different choices of α and β . (a) The existence of dimerization is established by choosing different system sizes N . (b) Dimer order parameters for different β . This parameter disappears for the critical $\beta=0.27$.

tion, the energy, and spin-spin correlation function have the same form as shown in Figs. 2 and 3. However it is worth mentioning that for Neel state of spin-2 chain, the corresponding dimer order parameter would be 8. Therefore our dimer order parameter is pretty small compared to strict antiferromagnets and the dimerization phase cannot be confirmed definitely. One possibility is the gap between excitation state and ground state for the present model is too small to be distinguished numerically. As a result, certain dimerized excitation state enters into our results and lead to such finite but tiny dimer order parameter. A promising solution is to apply the periodic boundary condition (PBC) here so that one can rule out the possibility of dimerization acquired from open boundary condition. Therefore, we have also done some calculation by DMRG for system with PBC. For the system size $N=100-200$ sites, we keep up to $m=3000$ states with truncation error smaller than 10^{-8} . Finally, we find that both OBC and PBC systems give us consistent results.

Observed the possible presence of dimerization, one can readily work out the phase diagram, see Fig. 5. The red curve stands for critical points of $|d^2E/d\alpha^2|$ while the two dashed dark curves are upper/lower bounds of dimerized phase of each β value. It shows the onset value for second-order derivative coincides with the upper bound of dimerized phase so that they describe the same phase transition between dimerized phase and SZH phase. While on the AKLT side, the phase transition would be of higher order that is invisible in Fig. 2. Despite the possible presence of dimerized phase,

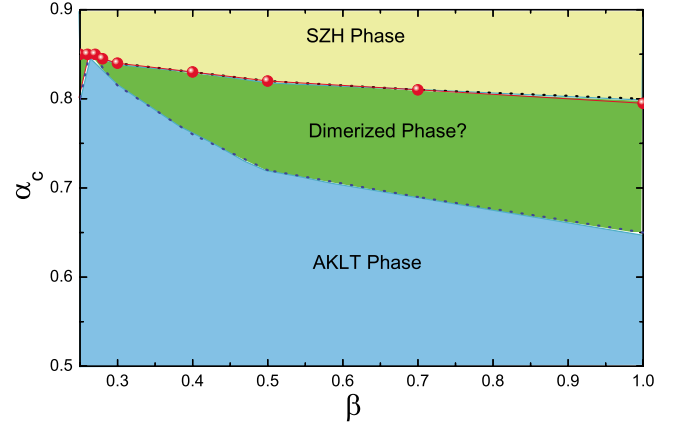


FIG. 5. (Color online) Ground-state phase diagram of the model Hamiltonian got by DMRG with $N=600$. The location of second-order phase transition for different β is indicated by the red line. The yellow region above red line belongs to SZH topological class while the light blue region belongs to AKLT class. Possible dimerization is shown in the green region sandwiched between these two phases.

the system undergoes a quantum phase transition without spontaneous breaking of translational symmetry at α_c when $\beta=0.27$. As the symmetry is unchanged in this case, this phase transition is originated from the topology only.

In conclusion, the topological distinction of the AKLT model and SZH model for the $S=2$ spin chain is presented in this work. A model Hamiltonian as an interpolation between these two models is introduced. The quantum phase transition of the model is protected by topology and established by DMRG calculation. The results indicate the presence of a dimered phase between two topological phases of AKLT and SZH. This dimered phase shrinks at critical value of $\beta_c=0.27$. One would like to realize this topological phase transition in real materials. On the AKLT side, we have a well-defined example already. $S=1$ edge spin is observed in $S=2$ chain of $\text{CsCr}_{1-x}\text{Mg}_x\text{Cl}_3$.²⁷ However, examples on SZH side are still missing. Probably one can employ cold atom techniques to realize TQPT proposed in this paper.

Recently, we became aware of a parallel work (Ref. 28) which has reached similar conclusions based on different approaches. They get a brilliant result about the universality class of phase transition but the possible dimer order phase is not mentioned.

We thank Zheng-Cheng Gu, Hosho Katsura, Naoto Nagaosa, and Yong-Shi Wu for insightful discussions. This work is supported by Ministry of Education of China under Grant No. B06011, the NSF of China, the National Program for Basic Research of MOST-China, and S.C.Z. is supported by the NSF under Grant No. DMR-0904264. H.C.J. acknowledges funding from Microsoft Station Q.

- ¹X.-L. Qi and S.-C. Zhang, *Phys. Today* **63**(1), 33 (2010).
- ²K. v. Klitzing, G. Dorda, and M. Pepper, *Phys. Rev. Lett.* **45**, 494 (1980).
- ³D. J. Thouless, M. Kohmoto, M. P. Nightingale, and M. den Nijs, *Phys. Rev. Lett.* **49**, 405 (1982).
- ⁴B. A. Bernevig, T. L. Hughes, and S. C. Zhang, *Science* **314**, 1757 (2006).
- ⁵C. L. Kane and E. J. Mele, *Phys. Rev. Lett.* **95**, 226801 (2005).
- ⁶F. D. M. Haldane, *Phys. Rev. Lett.* **61**, 1029 (1988).
- ⁷X. L. Qi, T. L. Hughes, and S. C. Zhang, *Phys. Rev. B* **78**, 195424 (2008).
- ⁸H. H. Tu, G. M. Zhang, and T. Xiang, *Phys. Rev. B* **78**, 094404 (2008).
- ⁹I. Affleck, T. Kennedy, E. H. Lieb, and H. Tasaki, *Phys. Rev. Lett.* **59**, 799 (1987).
- ¹⁰I. Affleck, T. Kennedy, E. H. Lieb, and H. Tasaki, *Commun. Math. Phys.* **115**, 477 (1988).
- ¹¹F. D. M. Haldane, *Phys. Rev. Lett.* **50**, 1153 (1983).
- ¹²D. Scalapino, S. C. Zhang, and W. Hanke, *Phys. Rev. B* **58**, 443 (1998).
- ¹³S. C. Zhang, *Science* **275**, 1089 (1997).
- ¹⁴E. Demler, W. Hanke, and S. C. Zhang, *Rev. Mod. Phys.* **76**, 909 (2004).
- ¹⁵C. Wu, J. P. Hu, and S. C. Zhang, *Phys. Rev. Lett.* **91**, 186402 (2003).
- ¹⁶A. Klümper, A. Schadschneider, and J. Zittartz, *J. Phys. A* **24**, L955 (1991).
- ¹⁷I. Affleck, D. P. Arovas, J. Marston, and D. Rabson, *Nucl. Phys. B* **366**, 467 (1991).
- ¹⁸D. Schuricht and S. Rachel, *Phys. Rev. B* **78**, 014430 (2008).
- ¹⁹D. P. Arovas, K. Hasebe, X. L. Qi, and S. C. Zhang, *Phys. Rev. B* **79**, 224404 (2009).
- ²⁰D. P. Arovas, A. Auerbach, and F. D. M. Haldane, *Phys. Rev. Lett.* **60**, 531 (1988).
- ²¹T. K. Ng, *Phys. Rev. B* **50**, 555 (1994).
- ²²X. G. Wen and Q. Niu, *Phys. Rev. B* **41**, 9377 (1990).
- ²³S. R. White, *Phys. Rev. Lett.* **69**, 2863 (1992).
- ²⁴A. Klümper, *J. Phys. A* **23**, 809 (1990).
- ²⁵M. T. Batchelor and M. N. Barber, *J. Phys. A* **23**, L15 (1990).
- ²⁶T. Kennedy and H. Tasaki, *Commun. Math. Phys.* **147**, 431 (1992).
- ²⁷H. Yamazaki and K. Katsumata, *Phys. Rev. B* **54**, R6831 (1996).
- ²⁸D. Zheng, G. Zhang, T. Xiang, and D. Lee, *arXiv:1002.0171* (unpublished).